Analysis of Inhomogeneously Filled Cavities Coupled to Waveguides Using the VIE Formulation

Andreas Jöstingmeier and A. S. Omar, *Senior Member, IEEE*

Abstract— **A method based on the volume integral equation (VIE) formulation is presented which can be used to analyze inhomogeneously filled cavities of arbitrary shape to which cylindrical waveguides of arbitrary cross section are coupled. The inhomogeneity inside the cavity is described by a spatially dependent permittivity. The method is applied to the problem of scattering by dielectric bodies inside waveguides. Furthermore, it will be demonstrated how the convergence of the method can be accelerated.**

I. Introduction

Of the variety of methods for the analysis of passive microwave components, only a few are capable of dealing with arbitrary inhomogeneities. Such versatile methods are e.g., the finite-difference [1], [2] and the finite-element [3], [4] methods operating in spatial domain. On the other hand, the VIE formulation is a generalized spectral-domain method because it is based on the expansion of the electromagnetic field with respect to suitable sets of eigenmodes. Hence, the VIE formulation can be seen as the spectral-domain counterpart of the infinite-difference and the finite-element methods. Other methods operating in the spectral-domain, like the mode-matching method [5], [6] or the conventional spectral-domain approach [7], [8], suffer from a lack of versatility concerning the treatment of an inhomogeneity with arbitrary space dependence.

In this paper, an inhomogeneously filled cavity which is coupled to two parallel waveguides (as shown in Fig. 1) will be considered. The extension to structures with more waveguides is straightforward. The fact that the inhomogeneity is modeled as a spatially dependent permittivity is another restriction which is not essential for the VIE formulation. A space-dependent permeability can be treated in the same way. The method can even be applied to inhomogeneities showing tensor character.

The VIE formulation is based on the expansion of the electromagnetic field inside the cavity with respect to complete sets of eigenmodes of the empty, short-circuited cavity [9]. These sets contain the divergence-free resonant modes as well as the curl-free eigenfunctions [10]. If instead of the electric field the divergence-free electric displacement is expanded, the curl-free electric field eigenfunctions need not be considered. On the other hand, the magnetic fields of the resonant modes are not sufficient for the expansion of the magnetic field. This can be explained by decomposing the structure into cavity and waveguides. According to the equivalence principle [11], the coupling apertures can be short circuited if the nonvanishing tangential electric field there is replaced by two surface magnetic currents at both sides of the short circuit. Due to these currents, the curl-free eigenfunctions are also necessary. Substituting the above described expansions into Maxwell's equations and expanding the electromagnetic fields in the apertures with respect to the waveguide eigenmodes, the expansion coefficients of the electromagnetic field inside the cavity are obtained in terms of the expansion coefficients of the electric fields in the apertures. Applying Galerkin's procedure, one gets, from the continuity of the tangential magnetic fields at the apertures, the cavity expansion coefficients in terms of those of the magnetic fields in the apertures. Eliminating the expansion coefficients of the cavity field, one arrives at a linear homogeneous system of equations relating the expansion coefficients of the magnetic fields in the apertures to those of the electric fields which is just the generalized admittance matrix of the cavity.

From another point of view, the VIE formulation is based on the expansion of an equivalent polarization current (the corresponding integral is taken over the volume of the cavity), the method presented here has been called "volume integral equation" formulation.

The analysis of the structure shown in Fig. 1 takes a lot of computational effort because, in general, all cavity eigen-

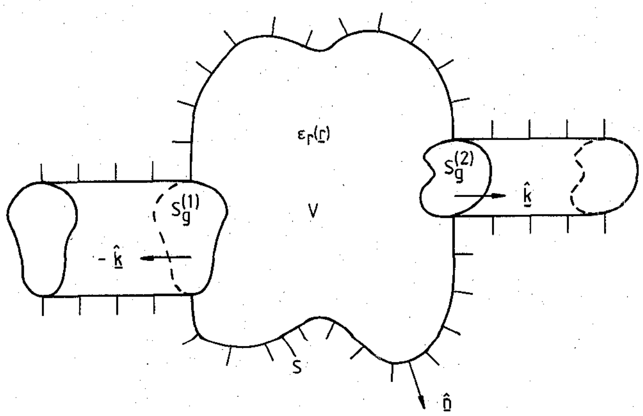

Fig. 1. Inhomogeneously filled cavity coupled to two parallel waveguides.

Manuscript received July 2, 1992; revised November 4, 1992. This work was supported by the Deutsche Forschungsgemeinschaft.

A. Jöstingmeier is with the Technische Universität Braunschweig, Insititut für Hochfrequenztechnik, Postfach 33 29, D-W-3300 Braunschweig, Germany.

A. S. Omar was with the Technische Universität Braunschweig, Insititut für Hochfrequenztechnik, Postfach 33 29, D-W-3300 Braunschweig, Germany. He is now with Technische Universität Hamburg-Harburg, Arbeitsbereich Hochfrequenztechnik, Postfach 90 10 52, D-W-2100 Hamburg 90, Germany.

IEEE Log Number 9209359.

modes are coupled by the spatially dependent permittivity. The computations can be simplified if we consider cylindrical waveguides containing cylindrical dielectric inserts according to Fig. 2. The general formulation will be applied to this case. Then all cavity eigenmodes of different axial orders are decoupled. In order to demonstrate the validity of the VIE formulations, we go even one step further and restrict the analysis to classes of field distributions which are decoupled from all other fields. Nevertheless, it will be shown how the numerical efficiency of the VIE formulation can be enhanced by some convergence accelerating procedures.

II. Theory

A. Basic Formulation

Let $\{\boldsymbol{E}_n\}$ and $\{\boldsymbol{H}_n\}$ denote the sets of electric and magnetic fields, respectively, corresponding to the resonant modes of the empty short-circuited cavity. The set of curl-free magnetic eigenfunctions will be denoted by $\{\boldsymbol{G}_n\}$. Then the following orthogonality relations hold:

$$\int_V \boldsymbol{E}_n \cdot \boldsymbol{E}_m^* \, dV = \delta_{nm} \frac{W_n}{\epsilon_0} \tag{1a}$$

$$\int_V \boldsymbol{H}_n \cdot \boldsymbol{H}_m^* \, dV = \delta_{nm} \frac{W_n}{\mu_0} \tag{1b}$$

$$\int_V \boldsymbol{G}_n \cdot \boldsymbol{G}_m^* \, dV = \delta_{nm} \frac{V_n}{\mu_0} \tag{1c}$$

$$\int_V \boldsymbol{H}_n \cdot \boldsymbol{G}_m^* \, dV = 0 \tag{1d}$$

where the asterisk $(*)$ and δ_{nm} denote complex-conjugate and the Kronecker delta, respectively. V denotes the volume of the short-circuited cavity. W_n and V_n are normalization quantities corresponding to field energies.

Due to the divergence-free nature of the electric displacement inside the cavity, the set $\{\boldsymbol{E}_n\}$ is sufficient for its expansion

$$\epsilon_r \boldsymbol{E} = \sum_n^\infty \frac{\omega_n}{\omega_0} a_n \boldsymbol{E}_n \tag{2a}$$

where ω_n and ω_0 are the resonance frequency of the nth resonant mode and a normalization frequency, respectively.

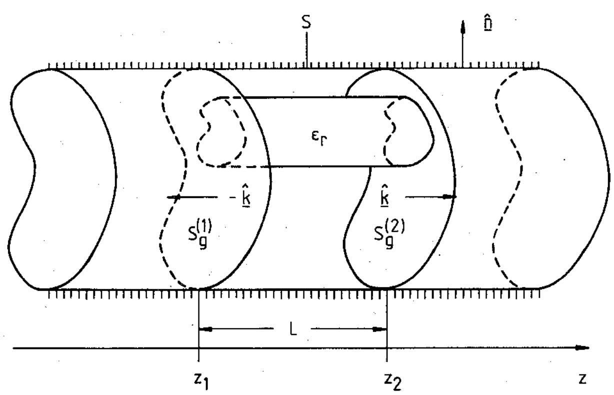

Fig. 2. Cylindrical waveguide containing a cylindrical dielectric insert.

For the expansion of the magnetic field, we have to take both sets $\{\boldsymbol{H}_n\}$ and $\{\boldsymbol{G}_n\}$ into account

$$\boldsymbol{H} = \sum_n^\infty c_n \boldsymbol{H}_n + \sum_n^\infty d_n \boldsymbol{G}_n . \tag{2b}$$

Substituting (2a) and (2b) into Maxwell's equations and making use of the orthogonality property of the cavity eigenmodes (1a)–(1d), one gets

$$c_n = \frac{\omega}{\omega_0} a_n \tag{3a}$$

$$\sum_m^\infty C_{nm} a_m - \left(\frac{\omega}{\omega_0}\right)^2 W_n a_n = \frac{1}{j\omega_0} \cdot \left(\int_{S_g^{(2)}} \left(\hat{\boldsymbol{k}} \times \boldsymbol{E}\right) \cdot \boldsymbol{H}_n^* \, dS - \int_{S_g^{(1)}} \left(\hat{\boldsymbol{k}} \times \boldsymbol{E}\right) \cdot \boldsymbol{H}_n^* \, dS \right) \tag{3b}$$

$$-\frac{\omega}{\omega_0} V_n d_n = \frac{1}{j\omega_0} \cdot \left(\int_{S_g^{(2)}} \left(\hat{\boldsymbol{k}} \times \boldsymbol{E}\right) \cdot \boldsymbol{G}_n^* \, dS - \int_{S_g^{(1)}} \left(\hat{\boldsymbol{k}} \times \boldsymbol{E}\right) \cdot \boldsymbol{G}_n^* \, dS \right) \tag{3c}$$

$$C_{nm} = \epsilon_0 \frac{\omega_n \omega_m}{\omega_0^2} \int_V \frac{\boldsymbol{E}_n^* \cdot \boldsymbol{E}_m}{\epsilon_r} \, dV \tag{3d}$$

where $\hat{\boldsymbol{k}}$ and $S_g^{(\nu)}$ are the unit vector in the axial direction and the coupling aperture between the cavity and the νth waveguide, respectively.

The aperture fields are expanded with respect to the eigenmodes of the waveguides. The transverse electric and the transverse magnetic fields in the aperture corresponding to the νth waveguide read

$$\boldsymbol{E}_t^{(\nu)} = \sum_i^\infty V_i^{e(\nu)} \nabla_t e_{zi}^{(\nu)} + \sum_i^\infty V_i^{h(\nu)} \left(\nabla_t h_{zi}^{(\nu)} \times \hat{\boldsymbol{k}}\right) \tag{4a}$$

$$\boldsymbol{H}_t^{(\nu)} = \sum_i^\infty I_i^{e(\nu)} \left(\hat{\boldsymbol{k}} \times \nabla_t e_{zi}^{(\nu)}\right) + \sum_i^\infty I_i^{h(\nu)} \nabla_t h_{zi}^{(\nu)} . \tag{4b}$$

The eigenmodes obey the orthogonality relations

$$\int_{S_g^{(\nu)}} \nabla_t e_{zi}^{(\nu)} \cdot \nabla_t e_{zj}^{(\nu)} \, dS = \delta_{ij} P_i^{e(\nu)} \tag{5a}$$

$$\int_{S_g^{(\nu)}} \nabla_t h_{zi}^{(\nu)} \cdot \nabla_t h_{zj}^{(\nu)} \, dS = \delta_{ij} P_i^{h(\nu)} \tag{5b}$$

$$\int_{S_g^{(\nu)}} \left(\nabla_t e_{zi}^{(\nu)} \times \nabla_t h_{zj}^{(\nu)}\right) \cdot \hat{\boldsymbol{k}} \, dS = 0 . \tag{5c}$$

The normalization quantities $P_i^{e(\nu)}$ and $P_i^{h(\nu)}$ describe the power flow of the ith TM and the ith TE eigenmode in the νth waveguide, respectively.

The aperture tangential electric fields are continuous

$$\hat{\boldsymbol{k}} \times \boldsymbol{E}\big|_{S_g^{(\nu)}} = \hat{\boldsymbol{k}} \times \boldsymbol{E}_t^{(\nu)}. \tag{6}$$

Substituting (6) and (4a) into (3b) and (3c) yields

$$\left([C] - \left(\frac{\omega}{\omega_0}\right)^2 [W]\right)\boldsymbol{a} = \left(\left[R^{e(2)}\right]\boldsymbol{V}^{e(2)} + \left[R^{h(2)}\right]\boldsymbol{V}^{h(2)} - \left[R^{e(1)}\right]\boldsymbol{V}^{e(1)} - \left[R^{h(1)}\right]\boldsymbol{V}^{h(1)}\right) \tag{7a}$$

$$-\frac{\omega}{\omega_0}[V]\boldsymbol{d} = \left(\left[S^{e(2)}\right]\boldsymbol{V}^{e(2)} + \left[S^{h(2)}\right]\boldsymbol{V}^{h(2)} - \left[S^{e(1)}\right]\boldsymbol{V}^{e(1)} - \left[S^{h(1)}\right]\boldsymbol{V}^{h(1)}\right) \tag{7b}$$

where $[C]$, $[W]$, and $[V]$ are a symmetric matrix with elements C_{nm} according to (3d) and diagonal matrices with elements according to (1a)–(1c), respectively. The quantities $\boldsymbol{a}$, $\boldsymbol{d}$, $\boldsymbol{V}^{e(\nu)}$, and $\boldsymbol{V}^{h(\nu)}$ are column vectors containing the elements a_n, d_n, $V_i^{e(\nu)}$, and $V_i^{h(\nu)}$, respectively. The matrices $\left[R^{e(\nu)}\right]$, $\left[R^{h(\nu)}\right]$, $\left[S^{e(\nu)}\right]$, and $\left[S^{h(\nu)}\right]$ containing the elements $R_{ni}^{e(\nu)}$, $R_{ni}^{h(\nu)}$, $S_{ni}^{e(\nu)}$, and $S_{ni}^{h(\nu)}$, respectively, represent the coupling between the waveguides eigenmodes and the cavity eigenmodes.

$$R_{ni}^{e(\nu)} = \frac{1}{j\omega_0}\int_{S_g^{(\nu)}} \left(\nabla_t e_{zi}^{(\nu)} \times \boldsymbol{H}_n^*\right) \cdot \hat{\boldsymbol{k}}\, dS \tag{8a}$$

$$R_{ni}^{h(\nu)} = \frac{1}{j\omega_0}\int_{S_g^{(\nu)}} \nabla_t h_{zi}^{(\nu)} \cdot \boldsymbol{H}_n^*\, dS \tag{8b}$$

$$S_{ni}^{e(\nu)} = \frac{1}{j\omega_0}\int_{S_g^{(\nu)}} \left(\nabla_t e_{zi}^{(\nu)} \times \boldsymbol{G}_n^*\right) \cdot \hat{\boldsymbol{k}}\, dS \tag{8c}$$

$$S_{ni}^{h(\nu)} = \frac{1}{j\omega_0}\int_{S_g^{(\nu)}} \nabla_t h_{zi}^{(\nu)} \cdot \boldsymbol{G}_n^*\, dS\,. \tag{8d}$$

The series representation of $\epsilon_r \boldsymbol{E}$ according to (2a) does not converge uniformly. The tangential electric fields of the short-circuited cavity eigenmodes vanish at the apertures $S_g^{(\nu)}$ which is not true for the original field. On the other hand, the series representation of the magnetic field according to (2b) converges uniformly. Hence, the boundary condition for the magnetic fields

$$\hat{\boldsymbol{k}} \times \boldsymbol{H}\big|_{S_g^{(\nu)}} = \hat{\boldsymbol{k}} \times \boldsymbol{H}_t^{(\nu)} \tag{9}$$

can be directly exploited by applying Galerkin's procedure. This yields

$$-j\omega_0\left(\left[R^{e(\nu)}\right]^\dagger \boldsymbol{c} + \left[S^{e(\nu)}\right]^\dagger \boldsymbol{d}\right) = \left[P^{e(\nu)}\right]\boldsymbol{I}^{e(\nu)} \tag{10a}$$

$$-j\omega_0\left(\left[R^{h(\nu)}\right]^\dagger \boldsymbol{c} + \left[S^{h(\nu)}\right]^\dagger \boldsymbol{d}\right) = \left[P^{h(\nu)}\right]\boldsymbol{I}^{h(\nu)}. \tag{10b}$$

The superscript † signifies the conjugate transpose of the corresponding matrix. $\left[P^{e(\nu)}\right]$, $\left[P^{h(\nu)}\right]$, and $\boldsymbol{I}^{e(\nu)}$, $\boldsymbol{I}^{h(\nu)}$ represent diagonal matrices and column vectors, respectively, containing the elements $P_i^{e(\nu)}$, $P_i^{h(\nu)}$, $I_i^{e(\nu)}$, and $I_i^{h(\nu)}$, respectively.

From (3a), (7a), (7b), (10a), and (10b), the cavity field expansion coefficients a_n, c_n, and d_n can be eliminated. This results in a linear system of equations relating the expansion coefficients of the transverse magnetic apertures fields to those of the transverse electric fields. The matrix equation represents the generalized admittance matrix of the structure

$$\begin{bmatrix} \boldsymbol{I}^{(1)} \\ \boldsymbol{I}^{(2)} \end{bmatrix} = \begin{bmatrix} \left[Y^{(11)}\right] & \left[Y^{(12)}\right] \\ \left[Y^{(21)}\right] & \left[Y^{(22)}\right] \end{bmatrix} \begin{bmatrix} \boldsymbol{V}^{(1)} \\ \boldsymbol{V}^{(2)} \end{bmatrix}. \tag{11a}$$

The matrix elements are given by

$$\left[Y^{(\nu\mu)}\right] = -(-1)^\mu j\omega \left[P^{(\nu)}\right]^{-1} \cdot \left(\left[R^{(\nu)}\right]^\dagger \left([C] - \left(\frac{\omega}{\omega_0}\right)^2 [W]\right)^{-1} [R^\mu] - \frac{1}{\left(\frac{\omega}{\omega_0}\right)^2}\left[S^{(\nu)}\right]^\dagger [V]^{-1}\left[S^{(\mu)}\right]\right). \tag{11b}$$

The matrices $\left[R^{(\nu)}\right]$, $\left[S^{(\nu)}\right]$, and $\left[P^{(\nu)}\right]$ combine the TM and the TE eigenmodes of the waveguides.

$$\left[R^{(\nu)}\right] = \left[\left[R^{h(\nu)}\right]\left[R^{e(\nu)}\right]\right] \tag{11c}$$

$$\left[S^{(\nu)}\right] = \left[\left[S^{h(\nu)}\right]\left[S^{e(\nu)}\right]\right] \tag{11d}$$

$$\left[P^{(\nu)}\right] = \begin{bmatrix} \left[P^{h(\nu)}\right] & [0] \\ [0] & \left[P^{e(\nu)}\right] \end{bmatrix}. \tag{11e}$$

The same holds for the column vectors $\boldsymbol{V}^{(\nu)}$, and $\boldsymbol{I}^{(\nu)}$

$$\boldsymbol{V}^{(\nu)} = \begin{bmatrix} \boldsymbol{V}^{h(\nu)} \\ \boldsymbol{V}^{e(\nu)} \end{bmatrix} \tag{11f}$$

$$\boldsymbol{I}^{(\nu)} = \begin{bmatrix} \boldsymbol{I}^{h(\nu)} \\ \boldsymbol{I}^{e(\nu)} \end{bmatrix}. \tag{11g}$$

The matrices $[C]$ and $[V]$ describe the coupling of the resonant modes and the curl-free eigenfunctions of the cavity by inhomogeneity, respectively. In general, all eigenmodes are coupled, which leads to large matrices and a lot of computation; but in the simpler case—when the cavity is a section of a waveguide which contains a cylindrical dielectric insert—the analysis is simpler.

B. Scattering by Dielectric Bodies Inside Waveguides

If the cavity is represented by a waveguide section according to Fig. 2, the eigenmodes of both waveguides to which the cavity is coupled are identical.

$$e_{zi} = e_{zi}^{(\nu)} \tag{12a}$$

$$h_{zi} = h_{zi}^{(\nu)}\,. \tag{12b}$$

In the transverse direction, the cavity eigenmodes can be formulated in terms of the waveguide eigenmodes; whereas in the axial direction, we have a sine or cosine dependence. Substituting the electric fields of the cavity eigenmodes into (3d) and taking the orthogonality property of sine and cosine into account, we obtain

$$C^{hh}_{in,jm} = \delta_{nm} \frac{\epsilon_0 L}{2} \frac{\omega^h_{in}\omega^h_{jn}}{\omega_0^2} \int_{S_g} \frac{\nabla_t h_{zi} \cdot \nabla_t h_{zj}}{\epsilon_r} \, dS \tag{13a}$$

$$C^{he}_{in,jm} = \delta_{nm} \frac{\epsilon_0 L}{2} \frac{\omega^h_{in}\omega^e_{jn}}{\omega_0^2} \frac{\left(\frac{n\pi}{L}\right)}{k^e_j} \int_{S_g} \frac{(\nabla_t e_{zj} \times \nabla_t h_{zi})}{\epsilon_r} \cdot \hat{k} \, dS \tag{13b}$$

$$C^{eh}_{in,jm} = \delta_{nm} \frac{\epsilon_0 L}{2} \frac{\omega^e_{in}\omega^h_{jn}}{\omega_0^2} \frac{\left(\frac{n\pi}{L}\right)}{k^e_i} \int_{S_g} \frac{(\nabla_t e_{zi} \times \nabla_t h_{zj})}{\epsilon_r} \cdot \hat{k} \, dS \tag{13c}$$

$$C^{ee}_{in,jm} = \delta_{nm} \frac{\epsilon_0 L}{2} \frac{\omega^e_{in}\omega^e_{jn}}{\omega_0^2} \cdot \left(\frac{\left(\frac{n\pi}{L}\right)^2}{k^e_i k^e_j} \int_{S_g} \frac{\nabla_t e_{zi} \cdot \nabla_t e_{zj}}{\epsilon_r} \, dS + (1+\delta_{n0}) k^e_i k^e_j \int_{S_g} \frac{e_{zi} e_{zj}}{\epsilon_r} \, dS \right) \tag{13d}$$

where ω^e_{in} and ω^h_{in} are the resonance frequencies of the TM and the TE cavity eigenmodes of transverse order i and axial order n, respectively.

$$\omega^h_{in} = c_0 \sqrt{\left(k^h_i\right)^2 + \left(\frac{n\pi}{L}\right)^2} \tag{14a}$$

$$\omega^e_{in} = c_0 \sqrt{\left(k^e_i\right)^2 + \left(\frac{n\pi}{L}\right)^2}. \tag{14b}$$

The cutoff wavenumbers of the ith TM and the ith TE waveguide eigenmodes are represented by k^e_i and k^h_i, respectively. c_0 and L denote the free-space velocity of light and the length of the cavity, respectively. In (13a), the superscript hh means that the coupling between two TE eigenmodes is considered. The meanings of the superscripts he, eh, and ee are similar. Note that in (13a)–(13d), all different axial orders are decoupled. Furthermore, the volume integral has turned into an integral over the cross section S_g of the waveguide.

The apertures and the waveguide cross section are identical. This leads to a lot of simplifications for the quantities describing the coupling between the cavity and the waveguide eigenmodes, some of which even vanish. This happens when the coupling between a TE cavity eigenmode and a waveguide eigenmode of TM type (and vice versa) is considered. Substituting these results and (13a)–(13d) into (11b), one arrives at

$$Y^{hh(\nu\mu)}_{ij} = -(-1)^\mu \left(\frac{j\omega P^h_j}{\omega_0^2 \mu_0^2} \sum_{n=1}^{\infty} \frac{\left(\frac{n\pi}{L}\right)^2}{\omega^h_{in}\omega^h_{jn}} D^{hh}_{in,jn} \cos(n\Theta) + \frac{k^h_i \delta_{ij}}{j\omega\mu_0} \frac{\cosh\left(k^h_i L \left(1 - \frac{\Theta}{\pi}\right)\right)}{\sinh\left(k^h_i L\right)} \right) \tag{15a}$$

$$Y^{he(\nu\mu)}_{ij} = -(-1)^\mu \frac{j\omega\epsilon_0 P^e_j}{\omega_0^2 \mu_0 k^e_j} \sum_{n=1}^{\infty} \left(\frac{n\pi}{L}\right) \frac{\omega^e_{jn}}{\omega^h_{in}} D^{he}_{in,jn} \cos(n\Theta) \tag{15b}$$

$$Y^{eh(\nu\mu)}_{ij} = -(-1)^\mu \frac{j\omega\epsilon_0 P^h_j}{\omega_0^2 \mu_0 k^e_i} \sum_{n=1}^{\infty} \left(\frac{n\pi}{L}\right) \frac{\omega^e_{in}}{\omega^h_{jn}} D^{eh}_{in,jn} \cos(n\Theta) \tag{15c}$$

$$Y^{ee(\nu\mu)}_{ij} = -(-1)^\mu \frac{j\omega\epsilon_0^2 P^e_j}{\omega_0^2 k^e_i k^e_j} \sum_{n=0}^{\infty} \omega^e_{in}\omega^e_{jn} D^{ee}_{in,jn} \cos(n\Theta) \tag{15d}$$

with

$$\Theta = \begin{cases} 0, & \nu = \mu \\ \pi, & \nu \neq \mu. \end{cases} \tag{15e}$$

The matrix

$$\begin{bmatrix} [D^{hh}] & [D^{he}] \\ [D^{eh}] & [D^{ee}] \end{bmatrix} = \begin{bmatrix} [C^{hh}] - \left(\frac{\omega}{\omega_0}\right)^2 [W^h] & [C^{he}] \\ [C^{eh}] & [C^{ee}] - \left(\frac{\omega}{\omega_0}\right)^2 [W^e] \end{bmatrix}^{-1} \tag{16}$$

has been introduced to allow a concise notation. The cavity normalization quantities W^e_{in}, W^h_{in}, and V_{in} can be expressed in terms of the waveguide normalization quantities P^e_i and P^h_i.

$$W^h_{in} = \frac{L\epsilon_0}{2} P^h_i \tag{17a}$$

$$W^e_{in} = \frac{L\epsilon_0}{2} \left(1 + \frac{\left(\frac{n\pi}{L}\right)^2}{\left(k^e_i\right)^2}\right) (1+\delta_{n0}) P^e_i \tag{17b}$$

$$V_{in} = \frac{L\epsilon_0}{2} (1+\delta_{n0}) P^h_i. \tag{17c}$$

In (11b), the influence of the curl-free eigenmodes is given by the term

$$-(-1)^\mu j\omega \left[P^{(\nu)}\right]^{-1} \frac{1}{\left(\frac{\omega}{\omega_0}\right)^2} \left[S^{(\nu)}\right]^\dagger [V]^{-1} \left[S^{(\mu)}\right].$$

The summation which is implied in this expression can analytically be evaluated leading to

$$-(-1)^\mu \frac{k^h_i \delta_{ij}}{j\omega\mu_0} \frac{\cosh\left(k^h_i L \left(1 - \frac{\Theta}{\pi}\right)\right)}{\sinh\left(k^h_i L\right)}$$

in (15a). The curl-free cavity eigenfunctions enter the hh part of the generalized admittance matrix only because the coupling between these eigenfunctions and the TM waveguide eigenmodes vanishes.

The computation of the generalized admittance matrix according to (15a)–(15d) is less CPU time and memory consuming than the general formulation. Due to the decoupling of the cavity eigenmodes of different axial orders, only a number of two-dimensional matrices (instead of one three-dimensional matrix) have to be inverted. The numerical efficiency, however, can still be enhanced by introducing some convergence accelerating procedures.

C. Convergence Acceleration

For the sake of simplicity, the analysis will be restricted to TE electromagnetic fields only in order to discuss the convergence accelerations. This restriction is possible because, for some structures, a subset of TE fields can be found which is decoupled from all other fields. Examples include the TE_{n0} fields in a rectangular waveguide containing a dielectric slab extending from top to bottom.

In implementing the formulation on a computer, all infinitely dimensioned matrices and infinite summations have to be truncated. For large orders, the matrix elements and the sum terms can be replaced by their asymptotic values. If a closed-form expression for a series with asymptotic sum terms or an analytic form of the inverse of an infinitely dimensioned matrix with asymptotic elements exists, the convergence can be accelerated considerably.

First the series of (15a) with respect to the axial order n should be examined. For our purpose, the series is reformulated

$$\sum_{n=1}^{\infty}\frac{\left(\frac{n\pi}{L}\right)^2}{\omega_{in}^h\omega_{jn}^h}D_{in,jn}^{hh}\cos(n\Theta)=\frac{2\omega_0^2}{\epsilon_0 L}\sum_{n=1}^{\infty}\frac{\left(\frac{n\pi}{L}\right)^2}{\left(\omega_{in}^h\right)^2\left(\omega_{jn}^h\right)^2}\overline{D}_{ij}^{hh(n)}\cos(n\Theta). \tag{18a}$$

For the matrix $[\overline{D}^{hh(n)}]$, with elements $\overline{D}_{ij}^{hh(n)}$, there holds

$$\left[\overline{D}^{hh(n)}\right]=\left(\left[Q^{hh}\right]-\omega^2\left[\Omega^{h(n)}\right]^{-2}\right)^{-1}. \tag{18b}$$

The matrix $\left[\Omega^{h(n)}\right]$ is a diagonal matrix containing the resonance frequencies ω_{in}^h

$$\Omega_{ij}^{h(n)}=\delta_{ij}\omega_{in}^h. \tag{18c}$$

The matrix $\left[Q^{hh}\right]$ with the elements

$$Q_{ij}^{hh}=\int_{S_g}\frac{\nabla_t h_{zi}\cdot\nabla_t h_{zj}}{\epsilon_r}\,dS \tag{18d}$$

describes the transverse coupling of the eigenmodes. It does not depend on the axial order n. For large n, $\omega^2/\left(\omega_{in}^h\right)^2$ behaves like $1/n^2$. In this case, $[\overline{D}^{hh(n)}]$ is approximately equal to $\left[Q^{hh}\right]^{-1}$. For a $\cos(n\Theta)/n^2$ dependence of the sum terms, a closed-form expression of the series exists. The final result is

$$\begin{aligned}\sum_{n=1}^{\infty}\frac{\left(\frac{n\pi}{L}\right)^2}{\omega_{in}^h\omega_{jn}^h}D_{in,jn}^{hh}\cos(n\Theta)\simeq\ &\frac{2\omega_0^2}{\epsilon_0 L}\sum_{n=1}^{N}\frac{\left(\frac{n\pi}{L}\right)^2}{\left(\omega_{in}^h\right)^2\left(\omega_{jn}^h\right)^2}\overline{D}_{ij}^{hh(n)}\cos(n\Theta)\\&+\left(\frac{L}{\pi c_0^2}\right)^2\left(\left[Q^{hh}\right]^{-1}\right)_{ij}\\&\cdot\left(\frac{\pi^2}{6}-\frac{\Theta}{4}(2\pi-\Theta)-\sum_{n=1}^{N}\frac{\cos(n\Theta)}{n^2}\right).\end{aligned} \tag{19}$$

The term

$$\frac{\pi^2}{6}-\frac{\Theta}{4}(2\pi-\Theta)$$

represents the closed-form expression of the asymptotic series from which

$$\sum_{n=1}^{N}\frac{\cos(n\Theta)}{n^2}$$

has to be subtracted because, in the range from $n=1$ to N, the asymptotic representation of the sum terms is not valid and the original series has to be computed.

Using (19), we expect rapid convergence as soon as the asymptotic representation of the sum terms is valid. Compared to the summation of the original series, the convergence acceleration leads to a strong reduction with respect to the number of sum terms which have to be taken into account.

In order to study the convergence with respect to the transverse order, we should look at the matrix inversion occurring in (18b). The convergence associated with the inversion of the infinitely dimensioned matrix is very slow. This means that even if a huge matrix is inverted, only a small part of $[\overline{D}^{hh(n)}]$ corresponding to the low transverse orders is approximately correct. The convergence can be accelerated if, instead of the numerical inverse of the truncated original matrix, the analytic inverse of an infinitely dimensioned matrix with asymptotic elements is considered.

For large transverse orders i, $\omega^2/\left(\omega_{in}^h\right)^2$ tends to zero. Hence, $[\overline{D}^{hh(n)}]$ is approximately given by

$$\left[\overline{D}^{hh(n)}\right]\simeq\begin{bmatrix}\left[Q_{11}^{hh}\right]-\omega^2\left[\Omega_{11}^{h(n)}\right]^{-2} & \left[Q_{12}^{hh}\right]\\ \left[Q_{21}^{hh}\right] & \left[Q_{22}^{hh}\right]\end{bmatrix}^{-1} \tag{20a}$$

with the submatrices

$$\left[Q_{11}^{hh}\right]=\left(Q_{ij}^{hh}\right)_{1\le i\le M,\,1\le j\le M} \tag{20b}$$

$$\left[Q_{12}^{hh}\right]=\left(Q_{ij}^{hh}\right)_{1\le i\le M,\,M<j<\infty} \tag{20c}$$

$$\left[Q_{21}^{hh}\right]=\left(Q_{ij}^{hh}\right)_{M<i<\infty,\,1\le j\le M} \tag{20d}$$

$$\left[Q_{22}^{hh}\right]=\left(Q_{ij}^{hh}\right)_{M<i<\infty,\,M<j<\infty} \tag{20e}$$

$$\left[\Omega_{11}^{h(n)}\right]=\left(\Omega_{ij}^{h(n)}\right)_{1\le i\le M,\,1\le j\le M}. \tag{20f}$$

Equation (20a) means that $\omega^2/\left(\omega_{in}^h\right)^2$ can be neglected in comparison to the diagonal elements of $\left[Q^{hh}\right]$ for $i>M$.

Evaluating the matrix inversion of (20a) with the submatrices defined in (20b)–(20f) leads to

$$\left[\overline{D}_{11}^{hh(n)}\right] \simeq \left(\left[Q_{11}^{hh}\right] - \left[Q_{12}^{hh}\right]\left[Q_{22}^{hh}\right]^{-1}\left[Q_{21}^{hh}\right] - \omega^2 \left[\Omega_{11}^{h(n)}\right]^{-2} \right)^{-1} \tag{21a}$$

where $\left[\overline{D}_{11}^{hh(n)}\right]$ denotes the upper left corner of $\left[\overline{D}^{hh(n)}\right]$.

$$\left[\overline{D}_{11}^{hh(n)}\right] = \left(\overline{D}_{ij}^{hh(n)}\right)_{1\le i\le M,\, 1\le j\le M}. \tag{21b}$$

Let us now consider the inverse of the infinitely dimensioned matrix $\left[Q^{hh}\right]$ consisting of the submatrices according to (20b)–(20e). The inverse of $\left[Q^{hh}\right]$ is correspondingly subdivided into the matrices $\left[Q_{11}^{hh,I}\right]$, $\left[Q_{12}^{hh,I}\right]$, $\left[Q_{21}^{hh,I}\right]$, and $\left[Q_{22}^{hh,I}\right]$.

$$\begin{bmatrix} \left[Q_{11}^{hh,I}\right] & \left[Q_{12}^{hh,I}\right] \\ \left[Q_{21}^{hh,I}\right] & \left[Q_{22}^{hh,I}\right] \end{bmatrix} = \begin{bmatrix} \left[Q_{11}^{hh}\right] & \left[Q_{12}^{hh}\right] \\ \left[Q_{21}^{hh}\right] & \left[Q_{22}^{hh}\right] \end{bmatrix}^{-1}. \tag{22a}$$

$\left[Q_{11}^{hh,I}\right]$ reads

$$\left[Q_{11}^{hh,I}\right] = \left(\left[Q_{11}^{hh}\right] - \left[Q_{12}^{hh}\right]\left[Q_{22}^{hh}\right]^{-1}\left[Q_{21}^{hh}\right] \right)^{-1}. \tag{22b}$$

Substituting (22b) into (21a) yields

$$\left[\overline{D}_{11}^{hh(n)}\right] \simeq \left(\left[Q_{11}^{hh,I}\right]^{-1} - \omega^2 \left[\Omega_{11}^{h(n)}\right]^{-2} \right)^{-1}. \tag{23}$$

Comparing (23) to the original equation (18b) shows that the convergence acceleration in the transverse direction can be carried out by simply replacing the truncated coupling matrix $\left[Q^{hh}\right]$ by the numerical inverse of its truncated analytical inverse $\left[Q^{hh,I}\right]^{-1}$.

In order to evaluate (19) and (23), it is necessary to know the inverse of the infinitely dimensioned matrix $\left[Q^{hh}\right]$. In [12], it has been proven that the analytical inversion of $\left[Q^{hh}\right]$ is obtained if one replaces ϵ_r^{-1} in (18d) by ϵ_r. Hence, for the elements of $\left[Q^{hh,I}\right]$, we get

$$Q_{ij}^{hh,I} = \int_{S_g} \epsilon_r \nabla_t h_{zi} \cdot \nabla_t h_{zj}\, dS. \tag{24}$$

The matrix $\left[Q^{hh}\right]$ does not appear in the formulation anymore. Therefore, only its inverse as given by (24) has to be calculated.

The application of (23) and (24) instead of the original relation (18b) leads to a strong reduction in the size of the transverse coupling matrix which is necessary in order to achieve convergence. This is especially important because the number of operations required for the inversion of an $(n \times n)$ matrix is proportional to n^3.

III. Numerical Results

Numerical results are computed for structures with the cross sections shown in Figs. 3 and 4. In describing microwave components, the scattering matrix is more common than the admittance matrix. Therefore, the generalized admittance matrix which we get from the analysis is transformed into the corresponding scattering matrix.

Fig. 3 shows the cross section of a circular waveguide containing a dielectric cylinder of length L. The azimuthally independent TE fields are decoupled from all other fields and can consequently be treated as a separate class. This follows from (13a)–(13d). In these equations, the integral over the cross section of the waveguide S_g can be decomposed into a radial and an azimuthal integration. Due to the rotational symmetry of the structure, all fields show a sine or cosine azimuthal dependence. Keeping the orthogonality property of these functions in mind, all fields of different azimuthal orders are decoupled. In addition, for azimuthally independent fields, TE and TM fields are not coupled because

$$(\nabla_t e_{zi} \times \nabla_t h_{zj}) \cdot \hat{\boldsymbol{k}}$$

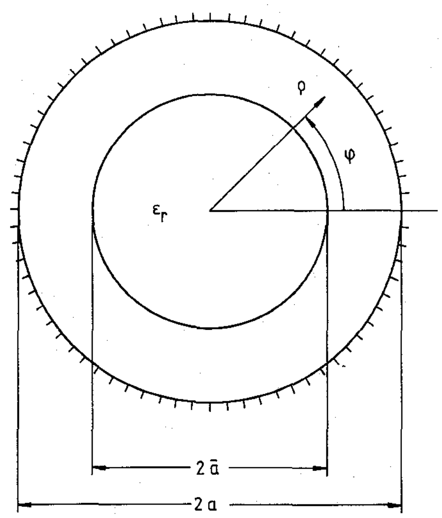

Fig. 3. Cross section of a circular waveguide containing a dielectric cylinder.

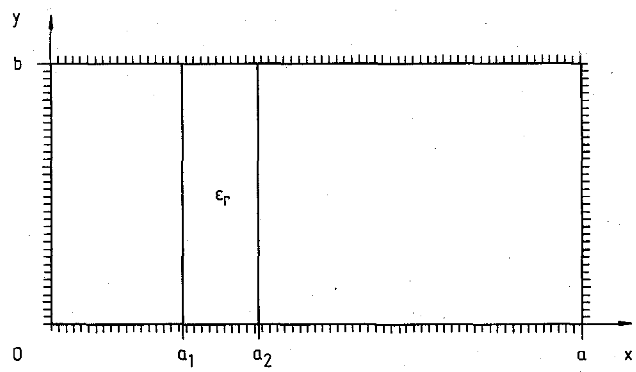

Fig. 4. Cross section of a rectangular waveguide containing a dielectric slab.

vanishes in this case. The elements of $[Q^{hh,I}]$ for azimuthally independent TE fields read

$$Q_{ij}^{hh,I} = \begin{cases} 1-\left(\frac{\overline{a}}{a}\right)^2(1-\epsilon_r)\dfrac{\left(1-\frac{1}{(k_i^h\overline{a})^2}\right)J_1^2(k_i^h\overline{a})+J_1'^2(k_i^h\overline{a})}{J_0^2(k_i^h a)}, & i=j \\ 2\frac{\overline{a}}{a^2}(1-\epsilon_r)\dfrac{k_j^h J_1(k_i^h\overline{a})J_1'(k_j^h\overline{a})-k_i^h J_1'(k_i^h\overline{a})J_1(k_j^h\overline{a})}{J_0(k_i^h a)J_0(k_j^h a)\left((k_j^h)^2-(k_i^h)^2\right)}, & i\neq j \end{cases} \tag{25}$$

where $\overline{a}$ and a denote the radii of the dielectric cylinder and the circular waveguide, respectively. J_0 and J_1 are the Bessel functions of order 0 and 1, respectively. The prime (′) means the derivative of the corresponding function with respect to its argument.

Fig. 5 shows the frequency dependence of the scattering parameters s_{11} and s_{12} for the H_{01} circular waveguide eigenmode. The frequency band extends from the cutoff frequency of this eigenmode to that of the next higher eigenmode. In this band, several resonances are observed. Comparing the results to those of a mode-matching method [13], the curves are so close together that differences cannot be seen.

The results of Fig. 5 have been achieved with a maximum transverse order $M = 20$ and a maximum axial order $N = 100$. The results do not change noticeably as long as $M \geq 10$ and $N \geq 10$ are maintained. Applying the formulation without convergence accelerations, even for $M = 50$ and $N = 200$, the results are not stable. This case requires approximately 2500 times more CPU time than the case with $M = 10$ and $N = 10$, which underscores the necessity for convergence accelerations.

In Fig. 4, a rectangular waveguide which contains a dielectric slab of length L is shown. For this structure, it can be proven that the y-independent TE fields are decoupled from other y-dependent fields. For this class, the elements of $[Q^{hh,I}]$ are given by

$$Q_{ij}^{hh,I} = \begin{cases} 1-(1-\epsilon_r)\left(\frac{a_2}{a}-\frac{a_1}{a}-\dfrac{\sin(2k_i^h a_2)-\sin(2k_i^h a_1)}{2k_i^h a}\right), & i=j \\ \frac{1}{a}(1-\epsilon_r)\left(\dfrac{\sin\left((k_i^h-k_j^h)a_1\right)-\sin\left((k_i^h-k_j^h)a_2\right)}{k_i^h-k_j^h}\right. \\ \qquad \left.-\dfrac{\sin\left((k_i^h+k_j^h)a_1\right)-\sin\left((k_i^h+k_j^h)a_2\right)}{k_i^h+k_j^h}\right), & i\neq j \end{cases} \tag{26}$$

where the coordinates a, a_1, and a_2 are defined in Fig. 4. Fig. 6 shows the frequency dependence of the scattering parameters for the H_{10} rectangular waveguide eigenmode. After studying the convergence of the results, statements which are similar to those valid for the circular waveguide structure can be made.

In Table I, the results of the VIE formulation are compared to those of two other methods [14], [15]. If we consider a dielectric slab with

$$\frac{L}{a} = \frac{a_2 - a_1}{a} << 1,$$

it should behave approximately like a circular dielectric post which has the same cross sectional area. In [14], this structure

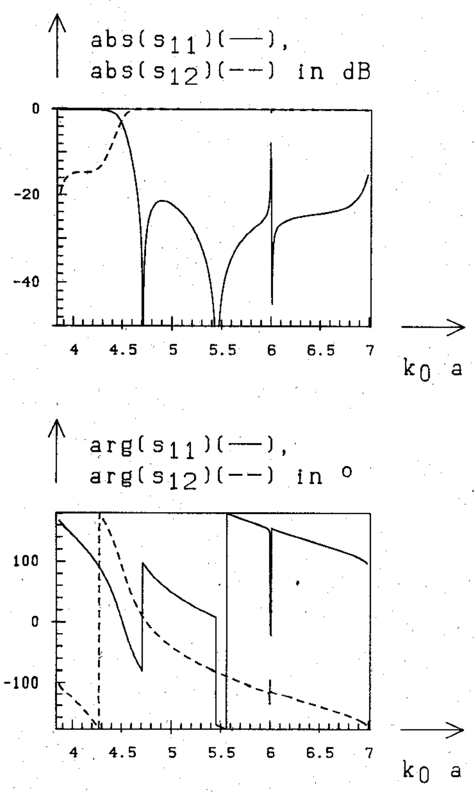

Fig. 5. Frequency dependence of the scattering parameters of the H_{01} eigenmode corresponding to the structure shown in Fig. 3 with $\overline{a}/a = 0.25$, $L/a = 0.5$, $\epsilon_r = 10$, $M = 20$, $N = 100$.

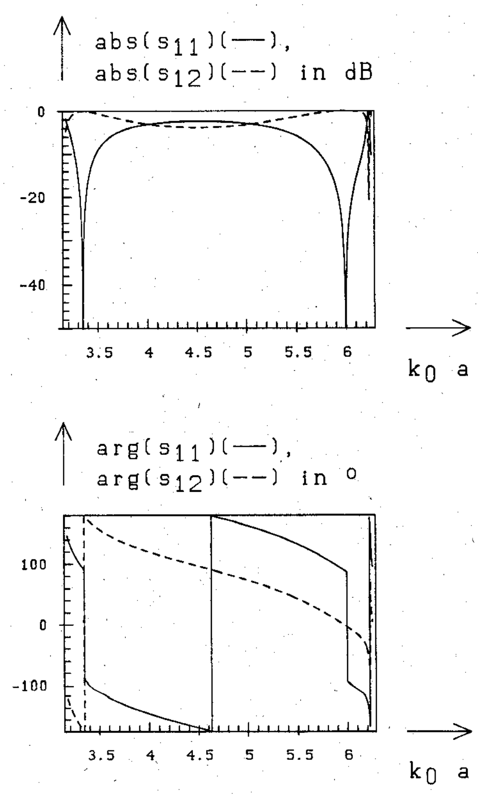

Fig. 6. Frequency dependence of the scattering parameters of the H_{10} eigenmode corresponding to the structure shown in Fig. 4 with $a_1/a = 0.25$, $a_2/a = 0.75$, $L/a = 0.5$, $\epsilon_r = 5$, $M = 20$, $N = 100$.

TABLE I
COMPARISON OF THE SCATTERING PARAMETERS OF THE VIE FORMULATION WITH THE RESULTS OF [14] AND [15] FOR THE STRUCTURE SHOWN IN FIG. 4 WITH $a_1/a = 0.45$, $a_2/a = 0.55$, $L/a = 0.1$, $\epsilon_r = 10$, $M = 50$, $N = 50$.

		VIE Formulation		Results from [14]		Results from [15]	
#	k_0a	$\|s_{11}\|$ in dB	$\|s_{21}\|$ in dB	$\|s_{11}\|$ in dB	$\|s_{21}\|$ in dB	$\|s_{11}\|$ in dB	$\|s_{21}\|$ in dB
1	3.173	−0.787	−7.807	−0.783	−7.825	−0.785	−7.815
2	3.515	−4.105	−2.137	−4.087	−2.148	−4.089	−2.147
3	3.857	−4.860	−1.717	−4.834	−1.730	−4.828	−1.733
4	4.199	−4.944	−1.677	−4.911	−1.693	−4.905	−1.695
5	4.541	−4.737	−1.778	−4.696	−1.799	−4.702	−1.796
6	4.883	−4.372	−1.975	−4.323	−2.004	−4.349	−1.989
7	5.266	−3.909	−2.266	−3.852	−2.305	−3.903	−2.270
8	5.568	−3.378	−2.672	−3.314	−2.726	−3.384	−2.667
9	5.910	−2.796	−3.236	−2.726	−3.314	−2.807	−3.224
10	6.252	−2.177	−4.043	−2.103	−4.159	−2.187	−4.028

is characterized by an equivalent circuit consisting of lumped elements; whereas in [15], a surface integral formulation has been applied. The results of the three methods are in good agreement, which proves the validity of the VIE formulation.

IV. CONCLUSIONS

Inhomogeneously filled cavities coupled to waveguides have been analyzed using a VIE formulation. In the basic formulation, the inhomogeneity inside the cavity may be an arbitrary function of space. It has been shown that the application of the method to scattering by dielectric bodies inside waveguides leads to several simplifications. In order to enhance the numerical efficiency of the formulation, convergence accelerating procedures have been discussed. Numerical results have been calculated for some structures. The validity of the method has been checked by comparing the results to those obtained by other methods. From the comparison of the computational requirements of the VIE formulation with and without convergence accelerations, it has been demonstrated that the numerical efficiency is drastically enhanced by the convergence accelerations.

REFERENCES

[1] G. Mur, "Finite difference method for the solution of electromagnetic waveguide discontinuity problems," *IEEE Trans. Microwave Theory Tech.*, vol. MTT-22, pp. 54–57, 1974.

[2] K. Bierwirth, N. Schulz, and F. Arndt, "Finite-difference analysis of rectangular dielectric waveguide structures," *IEEE Trans. Microwave Theory Tech.*, vol. MTT-34, pp. 1104–1114, 1986.

[3] B. M. A. Rahman and J. B. Davies, "Finite-element analysis of optical and microwave waveguide problems," *IEEE Trans. Microwave Theory Tech.*, vol. MTT-32, pp. 20–28, 1984.

[4] T. Angkaew, M. Matsuhara, and N. Kumagai, "Finite-element analysis of waveguide modes: A novel approach that eliminates spurious modes," *IEEE Trans. Microwave Theory Tech.*, vol. MTT-35, pp. 117–123, 1987.

[5] A. Wexler, "Solution of waveguide discontinuities by modal analysis," *IEEE Trans. Microwave Theory Tech.*, vol. MTT-15, pp. 508–517, 1967.

[6] T. S. Chu, T. Itoh, and Y.-C. Shih, "Comparative study of mode-matching formulations for microstrip discontinuity problems," *IEEE Trans. Microwave Theory Tech.*, vol. MTT-33, pp. 1018–1023, 1985.

[7] R. H. Jansen, "The spectral-domain approach for microwave integrated circuits," *IEEE Trans. Microwave Theory Tech.*, vol. MTT-33, pp. 1043–1056, 1985.

[8] Q. Zhang and T. Itoh, "Spectral-domain analysis of scattering from *E*-plane circuit elements," *IEEE Trans. Microwave Theory Tech.*, vol. MTT-35, pp. 138–150, 1987.

[9] A. S. Omar and K. Schünemann, "A new approach to the analysis of inhomogeneously filled cavities," in *Proc. 18th EuMC*, Stockholm, 1988, pp. 527–533.

[10] R. E. Collin, *Foundations for Microwave Engineering.* New York: McGraw-Hill, 1966.

[11] R. F. Harrington, *Time-Harmonic Electromagnetic Fields.* New York: McGraw-Hill, 1961.

[12] A. S. Omar and A. Jöstingmeier, "Analytical inversion of a class of infinitely dimensioned matrices encountered in some microwave problems," *IEEE Microwave Guided Wave Lett.*, vol. 2, pp. 316–318, 1992.

[13] ——, "Numerical results on dielectric resonators inside waveguides," in *Conf. Dig. 13th Int. Conf. Infrared Millimeter Waves,* Honolulu, HI, 1988, pp. 237–238.

[14] N. Marcuvitz, *Waveguide Handbook.* New York: McGraw-Hill, 1951.

[15] A. S. Omar and A. Jöstingmeier, "Application of the equivalence principle to the analysis of dielectric-loaded cavities coupled to waveguides," in *Conf. Dig. 15th Int. Conf. Infrared Millimeter Waves,* Orlando, FL, 1990, pp. 362–364.

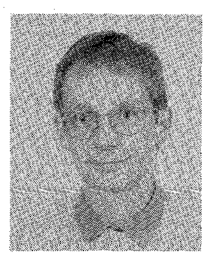

Andreas Jöstingmeier was born in Bielefeld, Germany, on May 25, 1961. He received the Dipl.-Ing. degree in electrical engineering from the Technische Universität Braunschweig, in 1987, and the Doktor-Ing. degree from the Technische Universität Hamburg-Harburg, Germany, in 1991.

Since 1991 he has been with the Institut für Hochfrequenztechnik at the Technische Universität Braunschweig as a Research Assistant. His current fields of research are concerned with numerical methods for microwave and millimeter-wave structures and high-power millimeter-wave tubes.